Beam Transport for Uniform Irradiation: Nonlinear Space Charge and the Effect of Boundary Conditions

D. Bruhwiler, Northrop Grumman Advanced Technology & Development Center, 4 Independence Way, Princeton NJ 08540[†]
Yuri K. Batygin, Moscow Engineering Physics Institute, 31 Kashirskoe shosse, 115409 Moscow, RUSSIA[*]

Proposed high-intensity ion accelerators required for Accelerator Driven Transmutation Technologies (ADTT) and the International Fusion Materials Irradiation Facility (IFMIF) demand careful control of beam shape and distribution on target; for example, uniform irradiation of a rectangular area. Nonlinear magnetic elements can yield the desired beam on target; however, nonlinear space charge forces also play a significant role. We consider the importance of boundary conditions used when modeling space charge effects in such a transport line. Simple analytical criteria are derived for determining when nonlinear space charge forces will be significant and for when proper treatment of boundary conditions is required. Two computer codes employing different boundary conditions for their respective space charge models, the PIC code BEAMPATH [1] and the high-order optics code TOPKARK [2], are used to simulate an example transport line in order to demonstrate our results.

I. BEAM INTENSITY REDISTRIBUTION

We consider a cylindrically-symmetric, unbunched beam of particles with charge q, mass m and current I, which propagates along the z-axis with velocity $v=\beta c$ and relativistic factor $\gamma=(1-\beta^2)^{-1/2}$. We assume the beam is space charge dominated, so that finite-emittance effects can be neglected.

In general, the space charge forces are nonlinear, so the density profile of the beam is changed nonlinearly along the z-axis. However, there is a distance where the different layers of the beam do not cross each other: the radial motion of the particles is nonlinear, but the beam flow is still laminar. Space charge forces distort the x-p_x phase space of a zero-emittance beam into an S-shape. The assumption of laminar flow holds as long as $p_x(x)$ remains a single-valued function.

For laminar flow, the number of particles contained in an arbitrary cylinder with initial radius r_o remains constant. Use of Gauss' theorem yields the result:

$$r\,E_r(r) \;=\; \frac{1}{\varepsilon_0}\int_0^{r_o} r'\,\rho(r')\,dr' \;=\; \text{const.} \tag{1}$$

Here, r is the radius of our hypothetical cylinder, which expands as the beam drifts; thus, r=r(z) and $r(z=0)\equiv r_o$.

We suppose the initial beam distribution to be Gaussian and define $R_0\equiv 2x_{rms}=2\langle x^2\rangle^{1/2}$:

$$\rho(r_o) \;=\; \frac{2I}{\pi R_0^2 \beta c}\,\exp\!\left(-2\,\frac{r_o^2}{R_0^2}\right) . \tag{2}$$

Use of Eq.'s (1) and (2) yields the radial space charge force at any location in z:

$$E_r(r) \;=\; \frac{I}{2\pi\varepsilon_0\beta c}\,\frac{f(r_o)}{r}\,; \qquad f(r_o)\equiv 1-\exp\!\left(-2\,\frac{r_o^2}{R_0^2}\right). \tag{3}$$

We note that for a uniform distribution, one would obtain $f(r_o) = (r_o/R_0)^2$, and R_0 would be the initial beam radius.

The equation of motion for a single particle in a drift region under the influence of space charge forces has the form:

$$\frac{d^2r}{dz^2} \;=\; \frac{2I}{I_0\beta^3\gamma^3}\,\frac{f(r_o)}{r}\;, \tag{4}$$

where $I_0\equiv 4\pi\varepsilon_0 mc^3/q$ is the characteristic current. Eq. (4) is the well-known envelope equation for a zero-emittance beam spreading in a drift region due to space charge [3], but here we apply it to the motion of a single particle within the beam.

If we define the following dimensionless variables

$$\bar{R} \;=\; \frac{r}{r_o}\;; \quad Z \;=\; \frac{z}{r_o}\sqrt{\frac{4\,I\,f(r_o)}{I_0\beta^3\gamma^3}}\quad , \tag{5}$$

then we can write the first integral of Eq. (4) in the form

$$\left(\frac{d\bar{R}}{dZ}\right)^2 - \left(\frac{d\bar{R}}{dZ}\right)^2_{init} \;=\; \ln\!\left(\bar{R}\right) . \tag{6}$$

Assuming the Z derivative of $\bar{R}$ vanishes initially, and for $1\le \bar{R}\lesssim 3$ ($0\le Z\lesssim 3.2$), Eq. (6) has the approximate solution [4]

$$\bar{R}(Z) \;\approx\; 1 + 0.25\,Z^2 - 0.017\,Z^3 . \tag{7}$$

This result is valid for a single particle, and it also describes how the radius of our hypothetical cylinder evolves with z.

The number of particles dN inside a thin ring (r, r+dr) is constant during the drift of the beam; hence, the particle density $\rho(r) = dN/(2\pi\, r\, dr)$ at any z is connected with the initial density $\rho(r_o)$ by the following equation [5]:

$$\rho(r) \;=\; \rho(r_o)\,\frac{r_o}{r}\frac{dr_o}{dr} \;=\; \rho(r_o)\,\frac{d(r_o^2)}{d(r^2)} . \tag{8}$$

Using Eq.'s (2), (7) and (8), we can write the beam distribution at any z location in the form

$$\rho(r) \;=\; \frac{(\,2\,I/\pi R_0^2\,\beta\,c\,)\,\exp(-2\xi_0^2)}{a_0 + a_1 F + a_2 F^2 + a_3 F^3 + a_4 F^4 + a_5 F^5 + a_6 F^6}\,, \tag{9}$$

where the following notation has been used:

$$\xi_0 = \frac{r_o}{R_0}\;; \qquad F(\xi_0) \;=\; \sqrt{\left[1-\exp(-2\xi_0^2)\right]/\,\xi_0^2}\;; \tag{10a}$$

$$\eta = \frac{4I}{I_0\beta^3\gamma^3}\,\frac{z^2}{R_0^2} = \frac{Z^2}{f(r_o)}\;; \quad a_0 = 1 + \eta\,\exp(-2\xi_0^2)\;; \tag{10b}$$

$$a_1 = -0.102\,\eta^{3/2}\exp(-2\xi_0^2);\;\; a_2 = \frac{1}{4}\eta^2\exp(-2\xi_0^2)\;; \tag{10c}$$

$$a_3 = 0.017\,\eta^{3/2} - 0.0425\,\eta^{5/2}\exp(-2\xi_0^2)\;; \tag{10d}$$

$$a_4 = 1.734\times 10^{-3}\,\eta^3\exp(-2\xi_0^2) - \frac{1}{16}\,\eta^2\;; \tag{10e}$$

$$a_5 = 0.01275\,\eta^{5/2}\;; \quad a_6 = -5.78\times 10^{-4}\,\eta^3 . \tag{10f}$$

The distribution is most uniform for $\eta\approx 4$. For larger values of η, the distribution becomes progressively more hollow.

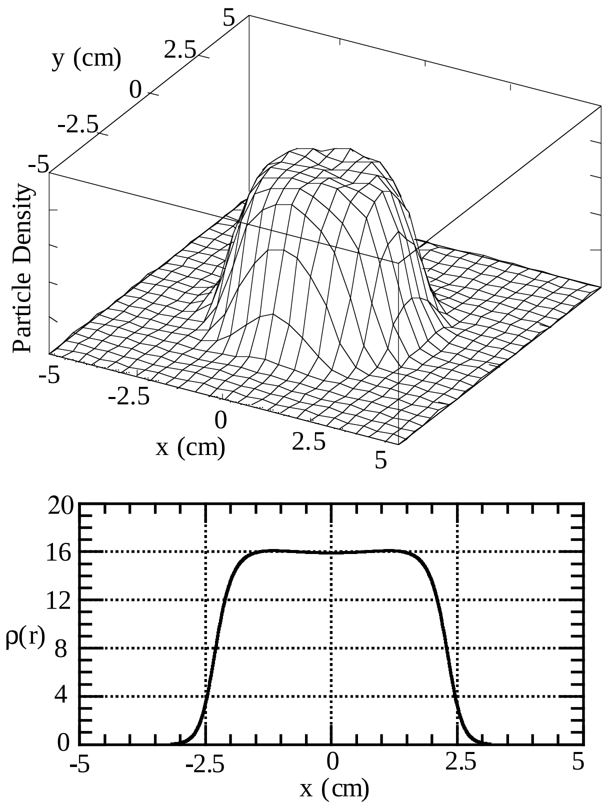

Figure 1: Initially Gaussian 2-D beam that has drifted under the influence of nonlinear space charge forces, with η=3.8; computer simulation above and analytical result below.

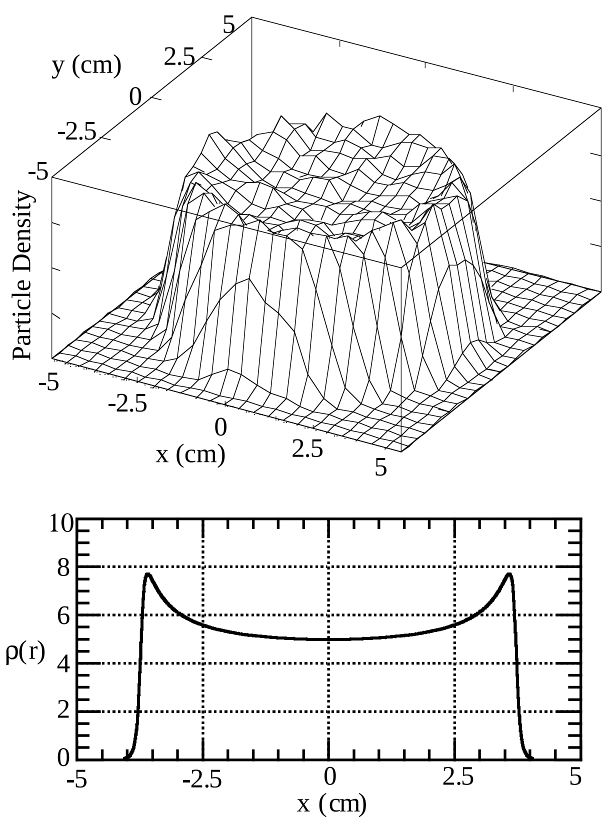

Figure 2: Same as Fig. 1, but for η=10; hollowing of the beam due to nonlinear space charge forces is shown.

Figures 1 and 2 show good comparison between theory and numerics for 35 MeV D^+ with I=4.7 A, R_0=1.3 cm and two values of η. BEAMPATH was used for the simulation, with 10^4 particles on a grid 256 x 256. Treatment of bunched beams requires the use of an equivalent peak beam current: $I= I_{bunch}*2\pi/\Delta\phi$, where $\Delta\phi$ is the phase length of the bunch.

II. GENERAL FEATURES OF THE CODES

BEAMPATH [1] is a PIC code advancing macroparticles on a 3-D rectangular grid of fixed dimensions with area-weighted charge distribution, using a combination of leap-frog and 2nd-order implicit methods. Space charge forces are found by solving Poisson's equation with FFT, imposing Dirichlet conditions at the transverse boundaries and longitudinal periodicity. For the simulation below, BEAMPATH used 10^4 particles and an x/2, y, z spatial grid of 128 x 256 x 128.

TOPKARK [2] is a ray-tracing code using a 4th-order Runge-Kutta integrator to advance an ensemble of particles. The Garnett and Wangler [6] ellipsoidal, Fourier-expansion space charge model is used to solve Poisson's equation with free-space boundary conditions. For the simulation below, TOPKARK used 10^4 particles and kept 10 Fourier modes.

III. LATTICE USED FOR CODE COMPARISON

The lattice considered here is one which bounces the beam first in y, and then in x. Octupole and duodecapole fields are applied at these waists in order to appropriately introduce nonlinearities into the two transverse phase planes with a minimum of x-y coupling. These nonlinearities result in a folding of the transverse phase plane distributions such that the final beam distribution f(x,y) on target is approximately constant with sharp boundaries. See Table I for details.

Table I. Nonlinear lattice for code benchmarking

ELEMENT	LENGTH	SETTING	
quadrupole	0.2 m	-10.16958	T/m
drift	0.4 m		
multipole	0.2 m	11.65657	T/m
octupole		-150.0	T/m^3
duodecapole		35000.0	T/m^5
drift	0.4 m		
quadrupole	0.1 m	0.91613	T/m
drift	0.4 m		
multipole	0.2 m	-11.90051	T/m
octupole		-80.0	T/m^3
duodecapole		0.0	T/m^5
drift	0.4 m		
quadrupole	0.2 m	10.78634	T/m
drift	17.5 m		

The design of such beamlines has been previously studied in some detail [5], [7]. Our primary objectives here are to 1) consider the effects of nonlinear space charge forces on beam transport through lattices of this type and 2) benchmark two codes with very different approaches to the problem of modeling space charge and with different boundary conditions. The distribution of the initial bunch was chosen to be Gaussian, truncated at 5 RMS. The FWHM and maximum excursion beam envelopes are shown in Fig. 3.

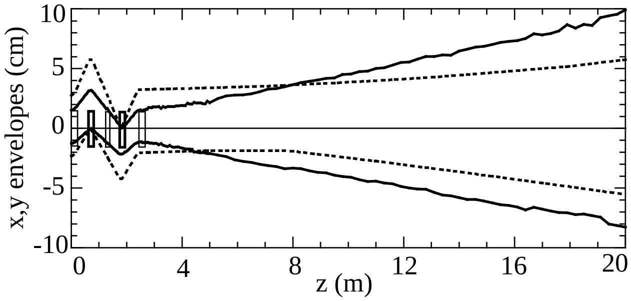

Figure 3: The FWHM (solid line) and maximum (dashed) x/y envelopes plotted above/below the axis.

IV. BOUNDARY CONDITIONS AND RESULTS

Consider a particle bunch in the beam frame with length z_b and radius r_b inside a perfectly conducting pipe of radius r_p. The impact of BC's on the space charge fields can be parameterized in terms of the geometry factor g [8]. Table I of Ref. [8] shows that for short bunches ($z_b \le r_b$) g in the presence of a perfectly conducting pipe differs significantly from the freespace g-factor g_0 only when r_b is comparable to r_p. However, for long bunches ($z_b >> r_b$) g can differ significantly from g_0 even when $r_p >> r_b$.

In the region containing magnetic lenses, the grid used in BEAMPATH is 10 cm in x and y (r_p~5 cm) and 8 cm in z. In this region, the transverse bunch width is typically 4 cm or less (r_b~2 cm), and the bunch length is short (z_b~1 cm). The resulting difference in the g-factors for the two codes should thus be at most a few percent. However, the maximum beam excursion does reach ~5 cm in x during the first multipole magnet and in y during the second multipole, so significant BC effects could arise in these two locations. In the long drift, the BEAMPATH grid is 20 cm in x and y (r_p~10 cm) and 32 cm in z. The bunch radius grows to $r_b \approx 5$ cm and the bunch length to $z_b \approx 10$ cm, so the maximum difference in the two g-factors should be ~20%. Differences resulting from the two types of longitudinal BC's have not yet been assessed.

In fact, the agreement between these two codes is remarkably close for this long, high-order, space-charge-dominated beamline. The beam phase space and space charge fields have been compared in detail at several critical points, showing only minor differences. We only have space to show the final x-y distribution in Fig. 4. TOPKARK was used to design the beamline and shows a very uniform beam. BEAMPATH shows a slightly hollow beam, which indicates slightly more nonlinear space charge fields due to differing BC's.

We chose a long lattice with high current to provide a rigorous comparison of the two codes, and applying the above analysis at the end of the last quadrupole yields $\eta \gtrsim 20 >> 4$. This beam is initially diverging and has finite emittance, so the assumptions of Section I do not hold; nevertheless, one would expect the final distribution to be hollow. TOPKARK simulations with no octupoles or duodecapoles do in fact yield a hollow beam. For this beamline, the nonlinear elements are required to partially counteract the space charge nonlinearities in order to obtain a uniform distribution on target.

VI. REFERENCES

† DLB acknowledges many useful discussions with M. F. Reusch, and the support of Northrop Grumman Corp.

* Present address: Inst. of Physical and Chemical Research (RIKEN), Hirosawa 2-1, Saitama 351-01, JAPAN

[1] Y. Batygin, "BEAMPATH: A program library for beam dynamics simulation in linear accelerators", Proc. of the 3rd European Part. Accel. Conf. (Berlin, 1992), p. 822.

[2] D. Bruhwiler and M. F. Reusch, "High-order optics with space charge: the TOPKARK code", AIP Conf. Proc. **297**, R. Ryne ed. (AIP, New York, 1993), p. 524.

[3] J. R. Pierce, in *Theory and Design of Electron Beams*, ed. by D. Van Nostrand (New York, 1954).

[4] S. I. Molokovskii and A. D. Sushkov, *Intense Electron and Ion Beams*, (Leningrad, Energia, 1972), in Russian.

[5] Y. K. Batygin, "Beam intensity redistribution in a nonlinear optics channel", Nucl. Instr. and Meth. B, **79** (1993), pp. 770-772.

[6] R. Garnett and T. Wangler, "Space-charge calculation for bunched beams with 3-D ellipsoidal symmetry", Part. Accel. Conf. Proc., (IEEE, New York, 1991), p. 330.

[7] B. Blind, "Production of uniform and well-confined beams by nonlinear optics", Nucl. Instr. and Meth. B, **57** (1991), pp. 1099-1102.

[8] C. Allen, N. Brown and M. Reiser, "Image effects for bunched beams in axisymmetric systems," Part. Accel. **45** (1994), pp. 149-165.

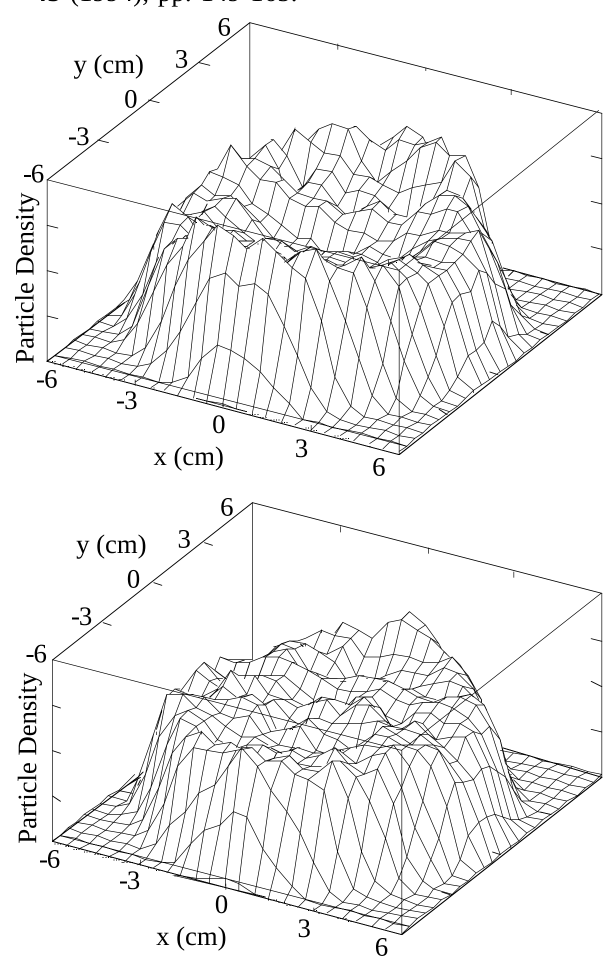

Figure 4. Final beam: BEAMPATH (above) and TOPKARK.